DIVERTOR STUDIES IN HELIOTRONS/TORSATRONS

V.Ye. Bykov, **V.V. Chechkin**, I.P. Fomin, L.I. Grigor'eva, A.V. Khodyachikh, N.I. Nazarov, R.O. Pavlichenko, V.G. Peletminskaya, V.V. Plyusnin, K.S. Rubtsov, V.A. Rudakov, A.I. Skibenko, M.S. Smirnova, E.L. Sorokovoj, V.S. Voitsenya, E.D. Volkov

Institute of Plasma Physics, National Science Center "Kharkov Institute of Physics and Technology", 310108 Kharkov, Ukraine

T. Mizuuchi, K. Nagasaki, H. Okada, A. Hayakawa, H. Funaba, T. Hamada, F. Sano, T. Obiki

Institute of Advanced Energy, Kyoto University, Gokasho, Uji 6110011, Japan

H. Zushi, M. Nakasuga, S. Besshou, K. Kondo

Graduate School of Energy Science, Kyoto University, Gokasho, Uji 6110011, Japan

S. Masuzaki, O. Motojima

National Institute for Fusion Science, Toki 5095292, Japan

1. Introduction

Diverted field lines (DFLs) are a natural element of a stellarator-type magnetic configuration, including heliotron/torsatron configuration. In particular, the existence of well formed bundles of DFLs and divertor flows (DFs) of plasma particles and heat in the l=2/m=19 Heliotron E (H-E) and l=3/m=9 Uragan-3M (U-3M) devices has been proved numerically and experimentally [1,2]. However, to create a valuable divertor facility for a future stellarator-like fusion reactor, a number of physical problems should be elucidated, some of most important ones being the effects on DFs of the real magnetic configuration and of different methods of heating. We present a review of experimental research on these subjects having been performed on H-E and U-3M.

Heliotron E

l=2, m=19

R=2.2 m, $\bar{a}$ ≈0.2 m, the inner radius of the rounded parts of the chamber is 0.41 m, the "X-point" structure is inside the chamber.

B_φ=1.9 T

Fundamental ECH (≤0.4 MW), 2nd harmonic ECH (≤0.3 MW), NBI, total P_{inj}≤3 MW

$\bar{n}_e \approx (1.0\text{-}2.5)\times 10^{19}$ m^{-3}

$T_e(0)\approx$0.6-1.5 keV, $T_i(0)\approx$0.3-0.6 keV

Diverted plasma is detected by 51 collector plates divided into 8 arrays arranged poloidally near the wall in 4 poloidal cross-sections Θ=0º/180º, 45º/225º, 90º/270º, 135º/315º, with plates 1,2,...,7 in each array

Uragan-3M

l=3, m=9

R=1m, $\bar{a}$ ≈0.12 m, the inner diameter of the helical coils is 0.19 m, the whole magnetic system is enclosed into a 5 m diameter vacuum chamber.

B_φ=0.4-1.0 T

Multimode Alfven heating, 5-8 MHz, $\omega\leq\omega_{ci}$, ≤0.5 MW, frame-like antenna A1, crankshaft antenna A2

$\bar{n}_e \approx (1\text{-}8)\times 10^{18}$ m^{-3}

$T_e(0)\approx$0.3 keV, $T_i(0)\approx$0.15 keV

Diverted plasma is detected by 2 arrays of 15 Langmuir probes installed at r=23 cm in the space between helical coils, the array 1 is behind the "X-point", the array 2 is between the OMS and the "X-point".

2. Heliotron E

2.1. Distribution of DFs, its asymmetry [3].The distributions of ion saturation current J_d in the plates 1,2,...,7 of each array are characterized by a strong up-down (i.e., vertical) asymmetry, contrary to what should be expected proceeding from the symmetry of the calculated connection length $L(\theta)$ distributions for the ideal H-E configuration (Fig. 1).

2.2. The effect of heating on DFs [3]. For all the heating regimes, the $J_d/\bar{n}_e$ parameter in the maxima of $L(\theta)$ is a rising function of $P_{abs}/\bar{n}_e$ where P_{abs} is the absorbed power (Fig. 2, the interpolating straight line is drawn for the NBI-only points). In the limit of small $P_{abs}/\bar{n}_e$ a finite $J_d/\bar{n}_e$ exists for all Θ, thus indicating an initial asymmetry, not depending on the heating. The initial asymmetry is enhanced as the heating power increases.

For some DFs, the $J_d/\bar{n}_e$ versus $P_{abs}/\bar{n}_e$ points obtained with participation of the fundamental ECH lie above the reference straight line in average (e.g., the flow *B*-0 in Fig. 2). This might be associated with a significant microwave power deposition at the periphery for this kind of heating [4].

2.3. Non-ambipolar divertor flows in H-E. In the most of divertor facilities the divertor plates are grounded. As the measurements show, the electric current to the grounded collector plates, J_p (plasma current) forms a complex distribution. In Fig. 3 the $J_d/\bar{n}_e$ versus $P_{abs}/\bar{n}_e$ dependence is shown for the pair of symmetrically disposed DFs *A*-90/*B*-270 as a characteristic example. It follows from Fig. 3 that a non-uniform poloidal distribution of the potential should arise in the SOL, thus generating parallel electric currents oppositely directed in the top and bottom parts of the torus. With the heating power increasing, the plasma currents reverse their direction in the top and bottom parts. The magnitude and the sign of $J_p/\bar{n}_e$ are governed mainly by $P_{abs}/\bar{n}_e$ rather than by the kind of heating and by the toroidal position of the heating power inlet. In particular, this means that J_p is determined by heating-induced processes occurring in the confinement volume.

3. Uragan-3M

3.1. DF distribution. The effect of RF heating. As the calculations have shown, there are two distinct peaks of the $L(\theta)$ distribution in the space between the helical coils on the line of probe array 1 disposition (Fig. 4(a)). The form of the ion saturation current J_s distribution depends substantially on the heating conditions. When the A2 antenna only is energized (the distance from the array 1 is >3 field periods, the main part of the irradiated power is deposited in the confinement volume), the J_s distribution agrees well with $L(\theta)$. If the antenna A1 (<1 field period, a significant amount of RF power is deposited in the SOL) is added to A2, a manifold J_s increase occurs in the vicinity of the probe 10 maximum. A predominant fraction of this DF is formed outside the OMS.

In accord with its position, the probe array 2 records a single maximum of J_s, its position being in a good agreement with that of the calculated $L(\theta)$ maximum (Fig. 4(b)).

3.2. Power dependence of DF [2]. With A2 in operation and $\bar{n}_e$ fixed, the current J_s in both maxima recorded by the array 1 is a rising function of RF power *P* irradiated by the antenna (Fig. 5). Under conditions with *P* and the hydrogen inlet fixed, the correlation between an enhanced $\bar{n}_e$ decay and an J_s rise in the vicinity of B_φ=0.45 T (Fig. 6) is one more evidence of the effect of power degradation of plasma confinement, as the fraction of *P* absorbed in the confinement volume is the largest at B_φ=0.45 T.

4. Summaries

1. Experimentally measured spatial distributions of diverted plasma flows can substantially differ in their magnitude and position from those, which are expected proceeding from the calculated distributions of the divertor field lines.

In the *l*=2 Heliotron E device, under NBI and ECH conditions a strong up-down asymmetry of DFs is observed. At least two factors seem to be responsible for this asymmetry: (1) a distortion of the magnetic structure of the divertor layer due to inaccuracies in manufacturing and installation of the helical coils resulting in an additional stochastization of the field lines in the SOL (by analogy with a double-null divertor in a tokamak [5]); (2) a vertical asymmetry of the helical magnetic field ripple in the top and bottom parts of the torus [6,7] resulting in a spatial re-distribution of groups of locally trapped high energy ions and electrons drifting vertically in opposite directions.

In the *l*=3 Uragan-3M device, to create and heat the plasma, RF fields are used generated by the antennae, which are crossed by the DFs. The proximity of the antenna to the probes and deposition of a fraction of RF power outside the OMS have a substantial effect on the measured DF distribution.

2. In both H-E and U-3M, the flow of diverted plasma increases with heating power irrespective of the kind of heating (NBI with different injection angles, fundamental and 2nd harmonic ECH, Alfven heating). The rate of DF increase seems to depend on the power deposition profile.

In whole, the DF increase with heating power can be considered as a manifestation of so-called power degradation of plasma confinement, the effect common for both tokamaks and stellarators [8].

3. In the H-E device, intense charge particle flows (electric currents) arise parallel to the diverted field lines. These currents always have opposite directions in the top and bottom parts of the torus, thus evidencing the existence of a poloidal electric field in the SOL plasma. The magnitude of any non-ambipolar DF is a rising

function of the total absorbed power and does not depend on the kind of heating and the toroidal position of the heating source in the first approximation. The above-mentioned vertical asymmetry of the helical magnetic field ripple resulting in the vertical drift of the locally trapped electrons and ions in opposite directions might be a possible reason for the observed spatial distribution of the non-ambipolar DFs.

References

[1] Obiki, T., et al., in Plasma Phys. and Control. Nucl. Fusion Res. 1988 (Proc. 12th Int. Conf. Nice, 1988), Vol. 2, IAEA, Vienna, 337 (1989).
[2] Bykov, V.Ye., et al., Plasma Phys. Control. Fusion **37** 271 (1995).
[3] Chechkin, V.V., et al., Distribution of Main Divertor Flows and Their Dependence on NBI and ECH in Heliotron E, Res. Rep. IAE-RR-98 056, Institute of Advanced Energy, Kyoto University, Uji, Japan (1998).
[4] Mizuuchi, T., at al., in Control. Fusion and Plasma Physics (Proc. 23d EPS Conf. Kiev, 1996), Vol. 20C, Part II, EPS, Geneva, 507 (1996).
[5] Marchand, R., et al., Nucl. Fusion **35** 297 (1995).
[6] Yushmanov, P.N., et al., Nucl. Fusion **33** 1293 (1993).
[7] Smirnova, M.S., Vertical Asymmetry of the Helical Field Ripple in Torsatrons/Heliotrons, Paper presented to Physics of Plasmas.
[8] Maassberg, H., et al., Plasma Phys. Control. Fusion **35** B319 (1993).

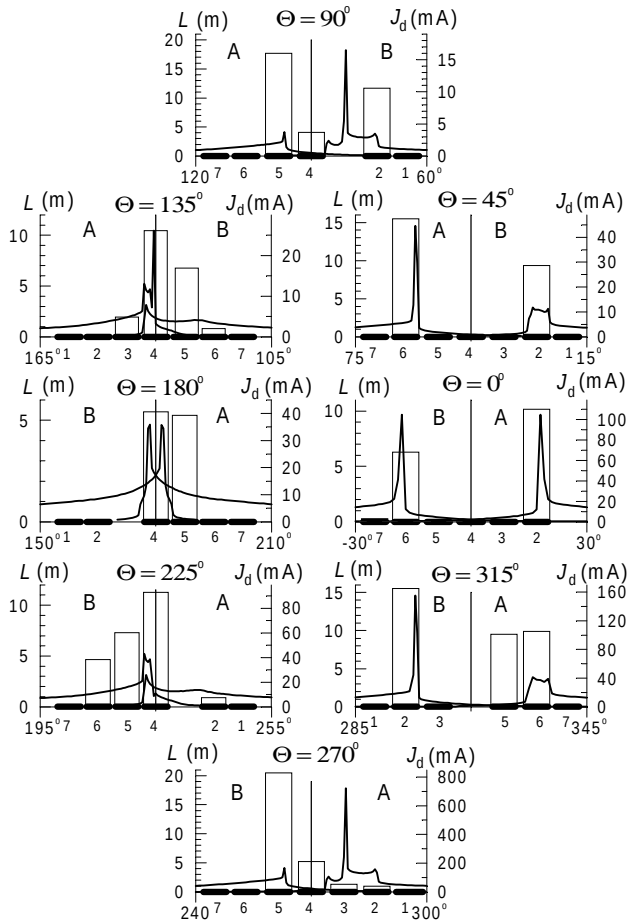

Fig. 1. *Poloidal distribution of connection length L (solid lines) and ion saturation current J_d (shaded rectangles) for different collector plate arrays Θ. A - in the B_φ direction; B - in the direction opposite to B_φ. NBI, P_{inj}≈0.7 MW; $\bar{n}_e$≈1.7×10^{19} m^{-3}.*

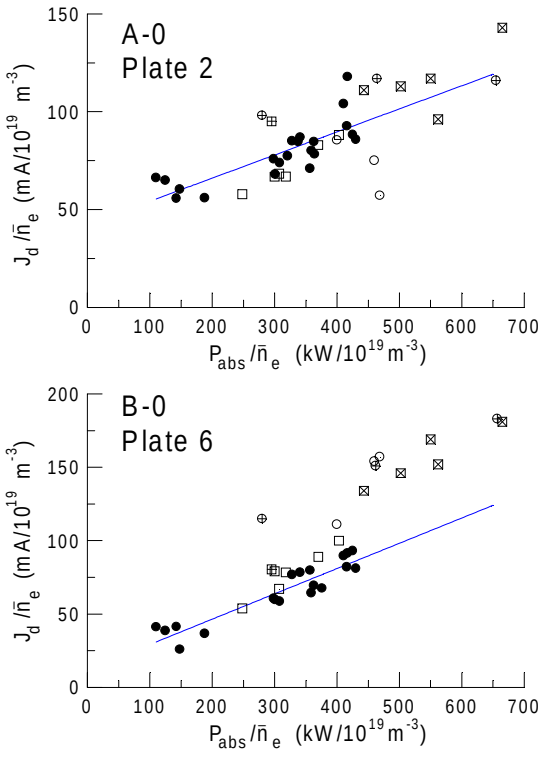

Fig. 2. *$\bar{n}_e$-normalized ion saturation current J_d in the divertor flows A and B at Θ=0° as a function of $\bar{n}_e$-normalized absorbed power P_{abs} in different regimes of plasma heating:NBI (●), fundamental ECH (○), 2nd harmonic ECH (□), NBI+fund. ECH (⊕), NBI+2nd harm. ECH (⊞), NBI+fund. ECH+2nd harm. ECH (⊠).*

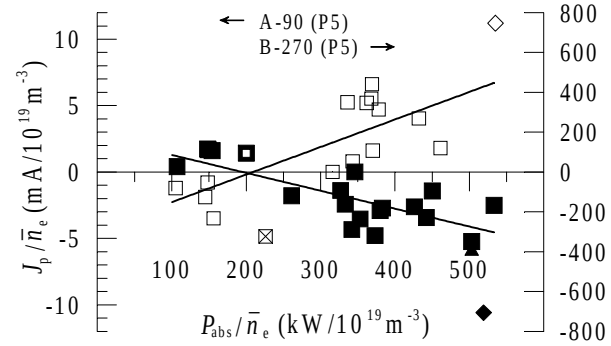

Fig. 3. *$\bar{n}_e$-normalized plasma current j_p as a function of $\bar{n}_e$-normalized absorbed power P_{abs} for the pair of symmetrically disposed divertor flows at $\Theta=90^o$ (flow A) and$\Theta=270^o$ (flow B) in different regimes of plasma heating: NBI (□,■), NBI BL-2+BL-5 (⊠,◘), NBI+ECH-1 (△,▲), NBI+ECH-1+ ECH-2 (◇,◆).*

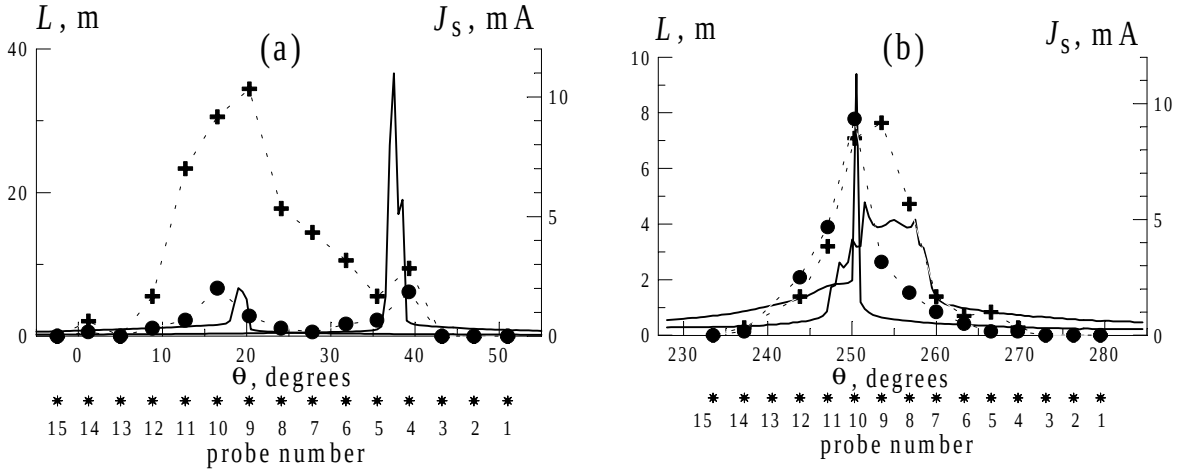

Fig. 4. *Calculated connection length L as a function of poloidal angle θ with the starting points lying on the lines of probe array 1 (a) and array 2 (b) disposition (solid lines). Ion saturation current J_s as a function of probe number: ● - A2; ✚ - A1+A2.*

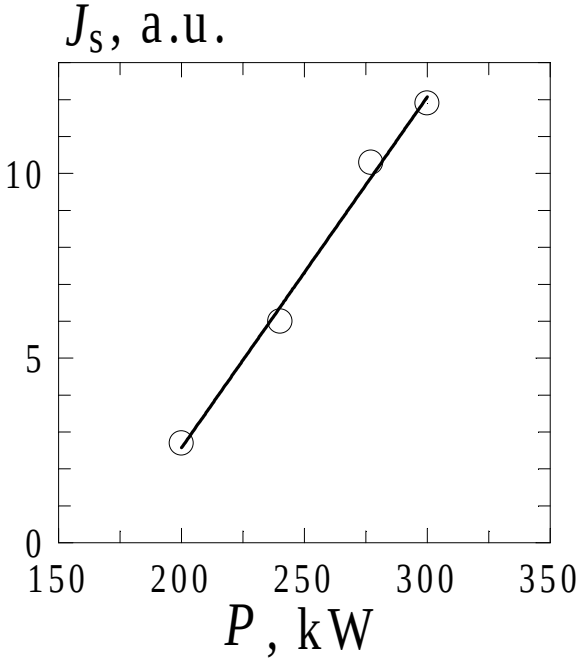

Fig. 5. *Ion saturation current J_s in the divertor flow as a function of RF power P with $\bar{n}_e$ fixed at a level of 2×10^{18} m^{-3}.*

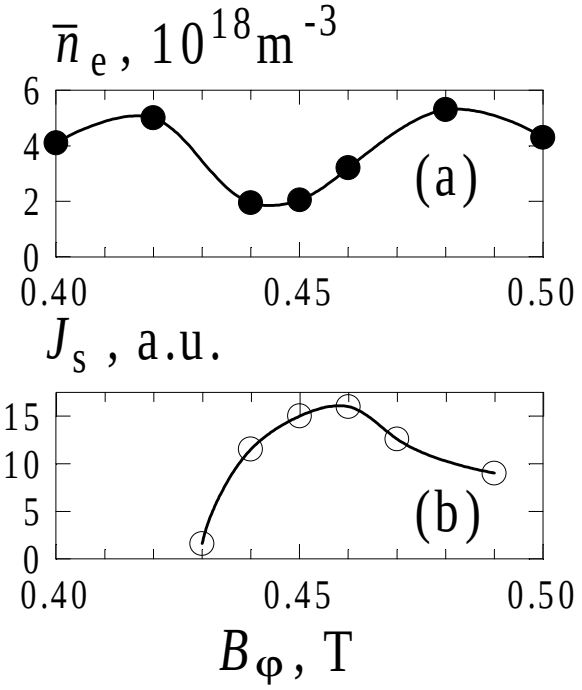

Fig. 6. *Electron density $\bar{n}_e$ (a) and ion saturation current in the divertor flow, J_s (b) as functions of B_φ at fixed values of RF power irradiated by antenna and hydrogen inlet.*